Transition of ductile and brittle fracture during DWTT by FEM

YouYou WU[1], Hailiang YU[1,2*], Cheng LU[1], Kiet TIEU[1], Ajit GODBOLE[1], Guillaume MICHAL[1]

[1] School of Mechanical, Materials & Mechatronic Engineering, University of Wollongong, NSW 2500, Australia
[2] School of Mechanical Engineering, Shenyang University, Shenyang, 110044, China
* Corresponding author: hailiang@uow.edu.au or yuhailiang1980@tom.com

Abstract Globally, steel pipelines are widely used to transport energy in the form of liquid petroleum and natural gas. The steel used in the manufacture of these pipelines must have high strength and toughness, and high resistance to fracture. The Drop Weight Tear Test (DWTT) is the most widely used test to assess brittle fracture characteristics in steel. The zones of ductile and brittle fracture during DWTT characterize the quality of pipeline steels. In this paper, the Gurson-Tvergaard-Needleman (GTN) fracture models are coupled in a Finite Element model. The ductile and brittle fracture zones in the samples are analyzed under different conditions. The results show that the change in fracture mode during the DWTT is from the brittle to the ductile, then again to the brittle. The calculated absorbed energies during DWTT compare well with experimental findings. Finally, we present an analysis of the transition from ductile to brittle fracture under different conditions.

Keywords Energy pipeline; ductile fracture; brittle fracture; DWTT

1. Introduction

Oil and gas provide 60% of the world's primary fuel and a large proportion is transported in pipelines. There is more than 33,000 km of high-pressure steel pipelines in Australia. The pipelines are designed, built and operated to well-established standards and rules, because the products they carry can pose a significant hazard to the surrounding population and environment. A combination of good design, adequate material properties and sound operating practices are therefore necessary, to ensure that transmission pipelines operate safely and efficiently.

Line pipe specifications specify minimum requirements for the shear area in a Drop Weight Tear Test (DWTT) to ensure the arrest of a long running brittle fracture. The DWTT, as specified in API RP 5L3 [1] or ASTM E436 [2], was developed by Battelle Memorial Institute in 1962 during the course of the American Gas Association NG-18 Research Program [3] to overcome some limitations of the Pellini drop-weight test which was developed by the US Naval Research Laboratory. In a DWTT, the test specimen is a rectangular bar with a length of 305 mm, a width of 76 mm and of the full material thickness (up to at least19mm). The specimen has a shallow pressed notch and is subjected to three-point bending, as shown in Fig. 1. The standards specify a 5 mm deep notch made by a sharp indenter with a 45° included angle resulting in a tip radius that is normally between 0.0127 to 0.0254 mm [1]. A series of specimens are broken under impact loading at various temperatures and the proportions of ductile fracture (shear) and brittle fracture (cleavage) on the fracture surfaces are measured. From correlations with full-scale pipe burst tests, a transition temperature corresponding to about 85 percent shear is normally defined in application standards as the fracture propagation transition temperature (FPTT) [4-5].

In this paper, a numerical method has been used to simulate the fracture behavior of pipelines. The most commonly used fracture model in computational fracture mechanics to characterize the toughness of line pipe steels is the modified Gurson model [6]. The Gurson model includes the influence of micro-voids on the plastic flow in a constitutive framework. The Gurson model was later modified extended by Tvergaard [7] and Needleman [8]. The modified Gurson- Tvergaard-Needleman(GTN) model is used to describe the acceleration of void growth. In this model, the

material is regarded as a continuum, composed of a ductile matrix with microvoids. There have been a limited number of studies applying this model to ductile materials [9-11].

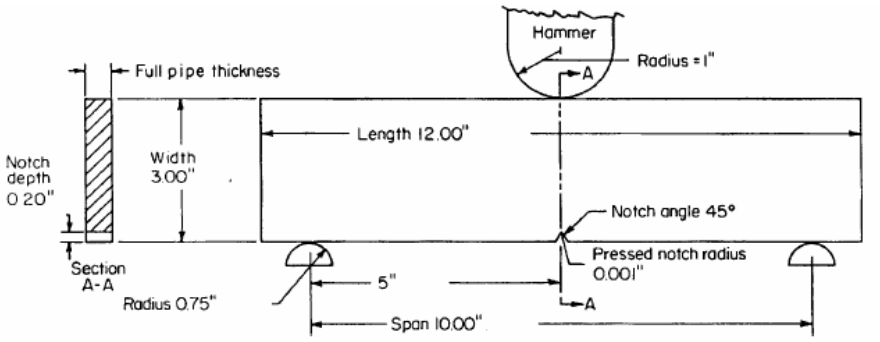

Fig. 1 Drop weight tear test (DWTT) specimen [2]

As opposed to simulations of the DWTT, simulations of Charpy tests are widely carried out to characterize the toughness of line pipe steels. Koppenhoefer and Dodds [12] investigated specimen size and loading rate effects on cleavage fracture of ferritic steels tested in the ductile-to-brittle transition region in pre-cracked Charpy specimens. The probability distribution for fracture of a cracked solid is defined by a two-parameter Weibull distribution [12]. Eberle et al. [13] developed 2D as well as 3D explicit dynamic finite element analyses, in combination with the rate-dependent Gurson model, to simulate Charpy tests. The simulated load-displacement curve and crack front are in close agreement with experimental observations. Tanguy et al. [14] conducted a numerical simulation of the Charpy V-notch test in the ductile-brittle transition regime using a modified Gurson-type model for ductile damage and Beremin model for cleavage fracture. Folch et al [15] also developed a local coupled brittle/ductile fracture approach model to predict either Charpy energy or fracture toughness and to investigate conditions for correlations between them using the Beremin and Gurson models. The modified Beremin model is based on the principles of Weibull statistics for the distribution of the defects and their size as is the standard Beremin model. The modified Gurson model, which incorporates a yield function for porous metal plasticity, was utilized in this work in conjunction with the Lemaitre and Beremin models. Thibaux and van den Abeele [16] reported on the fracture mechanics of instrumented Charpy tests performed on an X70 material. The tests were then simulated using a finite element method and the GTN constitutive model. Damage is represented by an internal variable, f, representing the void volume fraction which is assumed to be isotropic.

There have been very few reports on studies of the ductile-to-brittle transition region during a DWTT. Nonn et al [17] performed numerical simulations of a DWTT by applying the GTN model and compared the simulation results with experimental results from an instrumented DWTT. The results show that GTN model gives a reliable prediction of the load level variation with time when considering strain rate dependence. By applying GTN parameters validated on quasi-static fracture mechanics tests, the maximum load level including the beginning of the load drop for a DWTT can be well described quantitatively. The model equations were not provided in the publication.

In this paper, we used the GTN model to simulate the fracture behavior during DWTT. The stress at the notch was included as an initial condition in this model for the first time. The equivalent stress, nucleation of voids, void size distribution, etc, were analyzed. We found that the fracture propagates in a triangular shape at the crack tip, and the inverse fracture occurs when the fracture propagated about 3/4 of sample width in current study case. Some of the cases show that the transition during DWTT test is from the brittle to the ductile and then again to the brittle zone.

2. Models and simulation

The GTN damage model could be used to analyze the ductile fracture behavior under tension loads. In this paper, we also used the model to predict the damage behavior, as shown in Eq. (1),

$$\Phi = \frac{\sigma_{eq}^2}{\sigma_0^2} + 2q_1 f^* \cosh\left(-q_2 \frac{3p}{2\sigma_0}\right) - \left(1 + q_1^2 f^{*2}\right) \quad (1)$$

where p the hydrostatic pressure, σ_{eq} the effective Von Mises stress, σ_0 the yield stress of the matrix (function of the plastic deformation), q_1, q_2 are material parameters and f^* is the effective porosity. Material grade API 5L X80 was adopted in the models and the parameters are listed in Table 1.

Table 1 Main material parameters

Parameters	Value
Density, kg/m^3	7850
Young's Modulus, GPa	206
Yield stress, MPa	610
f^*	0.06
q_1,q_2	1.5,1.0

As specified in the ASTM E436 [2], the DWTT specimen is loaded in three-point bending by a drop hammer with 400kg weight and loading span of 254 mm. The simulated fracture test comprises two steps employed, as shown in Fig. 2: (1) pressing the notch and, (2) fracturing the sample under the action of the hammer. A three-dimensional geometrical model of the DWTT process was created with a pressed crack was set up with the above parameters and computational meshes with 8-node elements. The elements around the expected fracture zone are much finer than elsewhere in order to accommodate steeper gradients in parameters. In the models, there are 124864 elements and 127002 nodes. In the DWTT process, the hammer descends with an initial impact speed of 7 m/s.

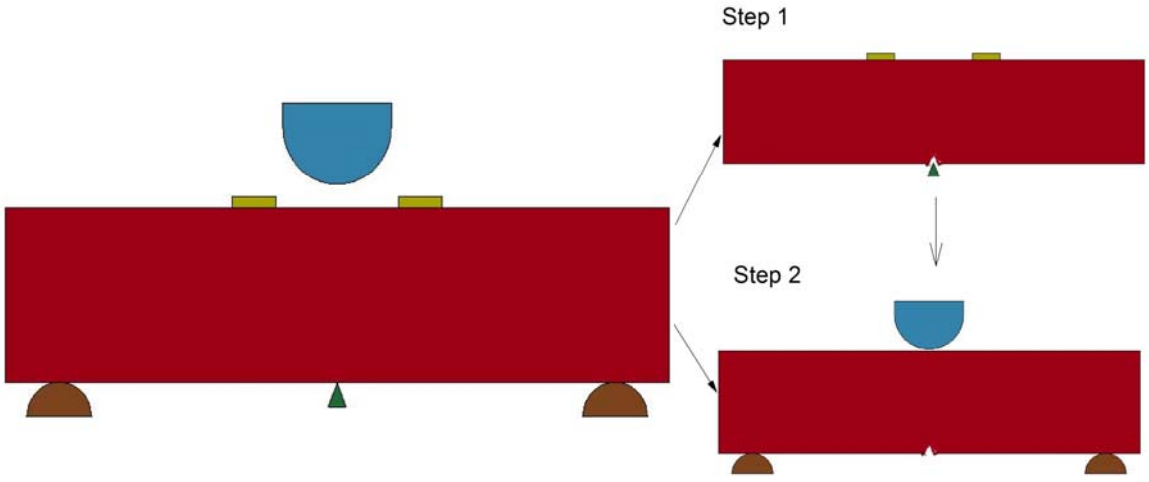

Fig. 2 Geometry of the full simulation process

3. Results and discussion

Fig.3 shows the equivalent stress distribution around the pressed notch position. After the pressed notch was introduced (step 1) at the centre of the specimen, stress concentration in the notch tip

area is observed prior to commencement of fracture. In the figure, we observe the maximum initial stress appeared in the notch tip zone, and this will affect the fracture behavior during the DWTT process.

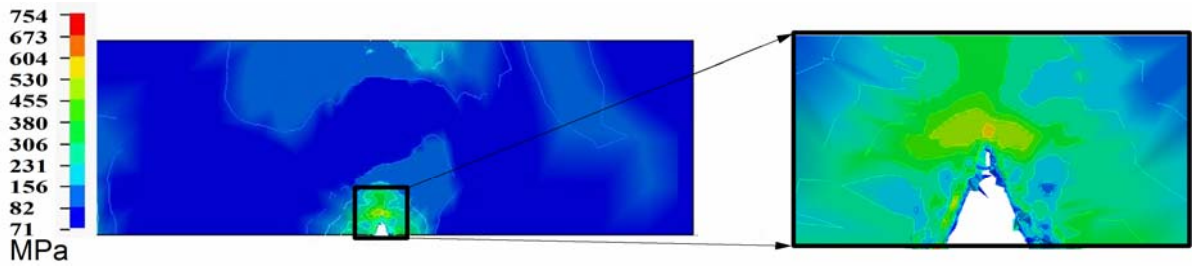

Fig. 3 Equivalent stress distribution and detail around the notch (MPa)

Fig.4 shows the equivalent stress distribution sequence during crack propagation (step 2). The equivalent stress is a three-dimensional stress calculated by Eq.(2). A maximum stress of 813 MPa is found at the notch tip and at the loading point, due to high stress concentration at these places. The stress value in the central area between the notch tip and the loading point is relatively small. A 'butterfly-wing' stress distribution is observed at the crack tip and at the loading point. The stress distribution is almost symmetrical about the loading line. As the crack propagates, the maximum stress distribution extends along the loading line till the specimen fractures.

$$\sigma_v = \sqrt{\frac{3}{2} s_{ij} s_{ij}} \tag{2}$$

Where S_{ij} are the components of the stress deviator tensor.

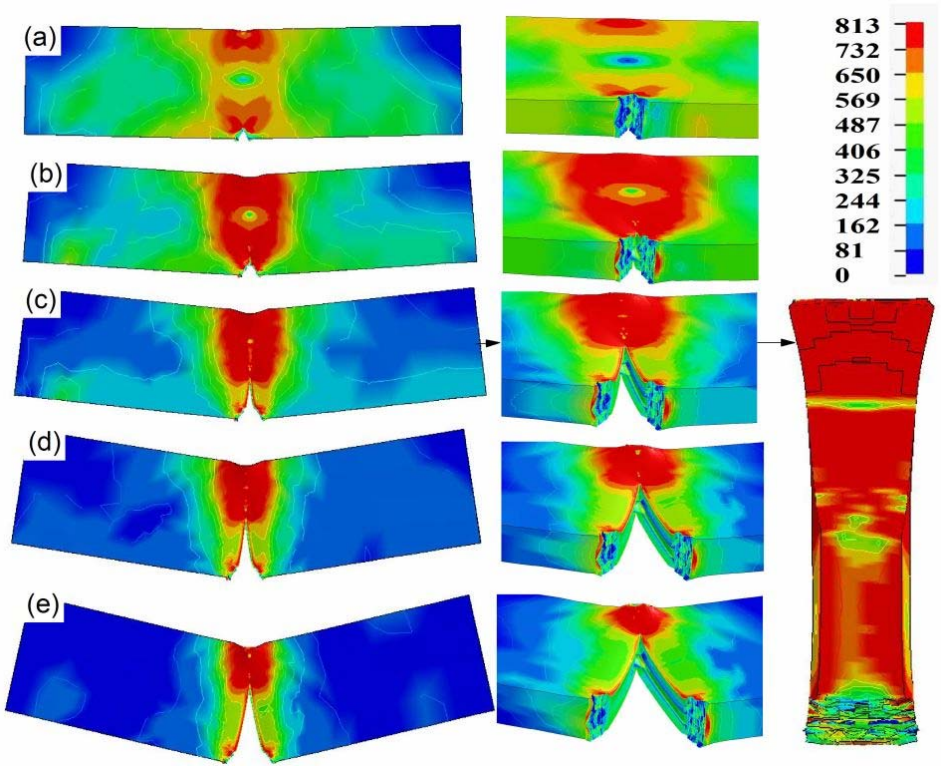

Fig.4 Equivalent stress distribution in DWTT sample (MPa)

Figure 5 shows the development of void nucleation during crack propagation from the notch tip to the impact side. The maximum void density always occurs at the two sides of the fracture surface where fully ductile fracture is seen. The voids appear to peak faster near the plane of symmetry. Which implies that the plasticity at the two sides of the sample is larger than that near the plane of symmetry.

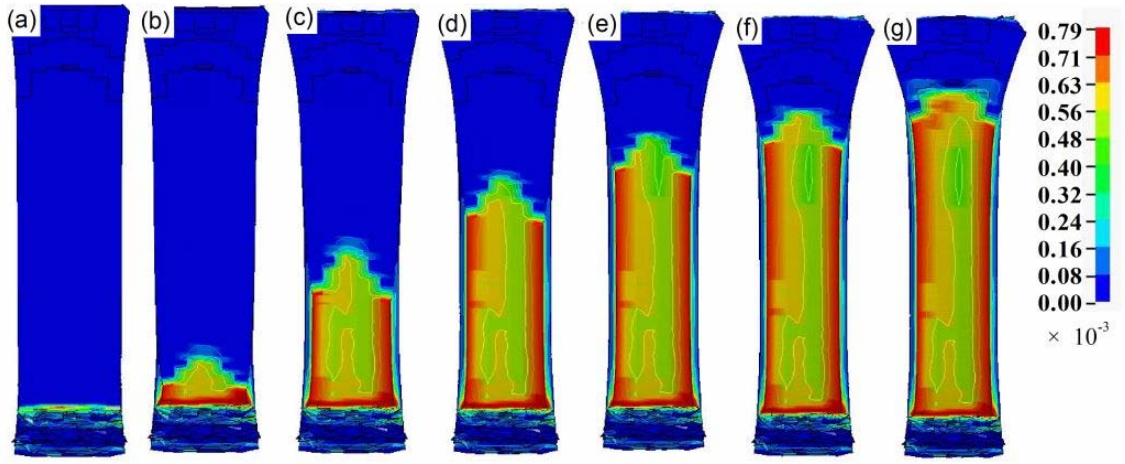

Fig.5 Nucleation of voids in DWTT samples

Fig.6 shows the void volume fraction distribution in the DWTT sample at different stages. It is seen that the void volume fraction in the pressed notch zone is slightly larger than in the other zone, suggesting that the process of notch pressing affects the initiation of fracture in the test sample. Hong et al. [18] concluded that the stress was less concentrated at the notch tip in the pressed-notch specimens compared to a Chevron notch, and this makes the initiation of fracture of pressed-notch specimens more difficult, and accordingly the deformation preceding the fracture initiation resulted in strain hardening in the hammer-impacted region increased.

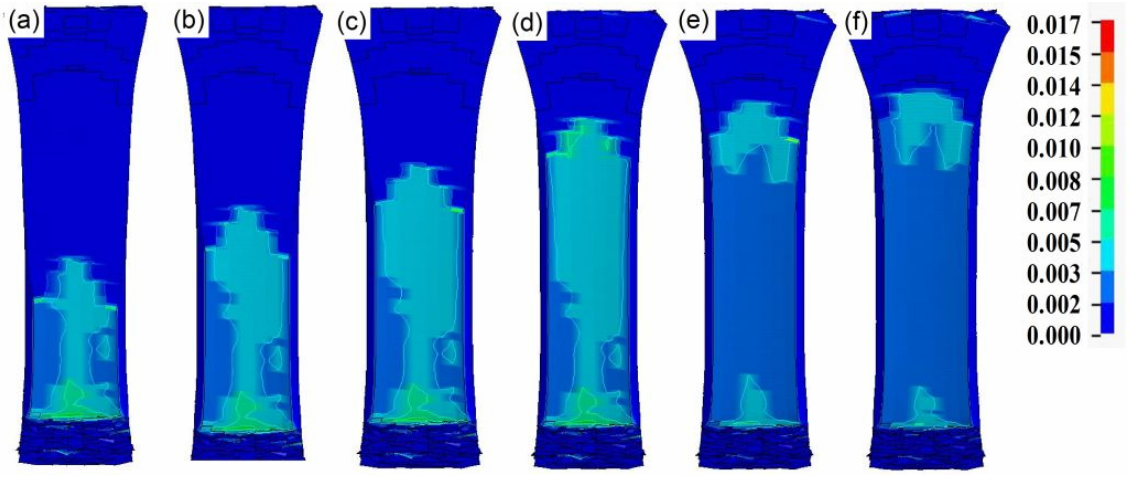

Fig. 6 Void volume fraction distribution in DWTT samples

As seen in Fig.7, the effective strain rate shows a peak near the plane of symmetry until the specimen fractures. This is consistent with the higher crack growth rate due to stress concentration near the surface of symmetry. As expected, the shape of effective strain rate distribution is found to be similar to the shape of the voids distribution. In Fig. 7 (g), it was observed that the inverse

fracture occurred when the fracture propagation reached 3/4 of sample width. The fracture also occurred at impact zones at same time.

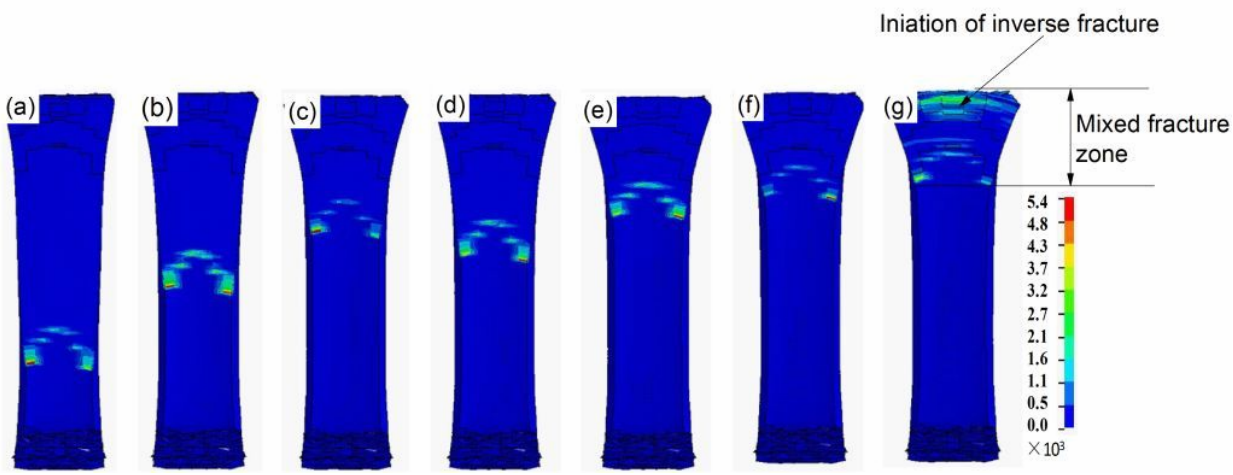

Fig. 7 Effective strain rate distribution in DWTT samples (s^{-1})

The appearance of the simulated fracture surface is in close agreement with the experimental results [18] in terms of stress distribution and fracture morphology as shown in Fig.8. Fracture was initiated as cleavage fracture followed by shear fracture, and then an inverse fracture occurred at the impact zone of the sample. Further analyses on ductile-brittle transition will be carried out by developing a coupled brittle/ductile fracture model in the near future. The relationship between the initiation of inverse fracture and the length of mixed fracture zone need to be further investigated.

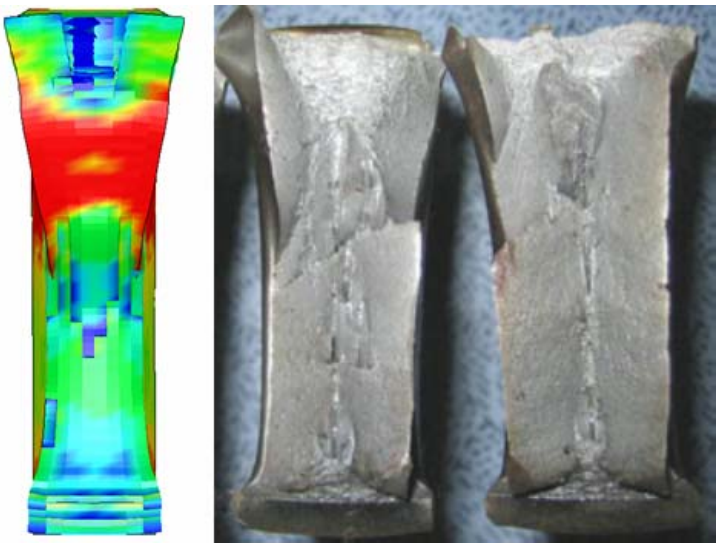

Fig. 8 Simulated results versus the experimental results obtained in ref 18.

4. Conclusions

(1) A finite element model using the Gurson-Tvergaard-Needleman damage model was employed to simulate the fracture process of pipeline steel during DWTT, in particular, considering the state of initial stress around the pressed notch.

(2) During DWTT, the fracture follows a triangular shape in the sample due to higher constraint at

the mid-thickness. This is compatible with the simulation results for void nucleation distribution and effective strain rate distribution.

(3) The simulated results are in good agreement compared with the experimental results in terms of stress distribution and fracture morphology. The relationship between the initiation of inverse fracture and the length of mixed fracture zone need to be further investigated.

Acknowledgements

The authors appreciate Prof. Valerie Linton (Energy Pipeline CRC), Dr. John Piper (John Piper & Associates) and Leigh Fletcher (Welding and Pipeline integrity) for the suggestions in revision of the manuscript.

This work was funded by the Energy Pipeline CRC, supported through the Australian Government's Cooperative Research Centre Program. The funding and in-kind support from the APIA RSC is gratefully acknowledged.

The corresponding author gratefully acknowledges the financial support from the Vice-Chancellor's Fellowship Grant at the University of Wollongong, the National Natural Science Foundation of China through Grant 51105071 and the Doctorate Foundation of the Ministry of Education of China through the Grant 20090042120005.

References

[1] ANSI/API, Recommended Practice for Conducting Drop-Weight Tear Tests on Line Pipe, Third Edition, 1996.
[2] ASTM, Standard Test Method for Drop-Weight Tear Tests of Ferritic Steels, 2008.
[3] A. Cosham, D. G. Jones, R. Eiber, P. Hopkins, Don't drop the drop weight tear test. Journal of Pipeline Engineering, 9(2010).69-84.
[4] R. J. Eiber, B. N. Leis, Fracture control technology for natural gas pipelines circa 2001, Report No. PR-003-00108 to PRCI, 2001.
[5] R. J. Eiber, Correlation of full scale tests with laboratory tests. 3rd Symposium on Line Pipe Research, American Gas Association, November 1965, 83-118.
[6] A. L. Gurson, Continuum theory of ductile rupture by void nucleation and growth: part i---yield criteria and flow rules for porous ductile media. Journal of Engineering Materials and Technology, 99(1977) 2-15.
[7] V. Tvergaard, Influence of voids on shear band instabilities under plane strain conditions. International Journal of Fracture, 17 (1981) 389-407.
[8] V. Tvergaard, A. Needleman, Analysis of the cup-cone fracture in a round tensile bar, Acta Metallurgica, 32(1984) 157-169.
[9] G. Bernauer, W. Brocks, Micro-mechanical modelling of ductile damage and tearing – results of a European numerical round robin. Fatigue & Fracture of Engineering Materials & Structures, 25 (2002) 363-384.
[10] C. Ruggieri, T.L. Panontin, R.H. Dodds, Numerical modeling of ductile crack growth in 3-D using computational cell elements, International Journal of Fracture, 82 (1990) 67-95.
[11] X. Gao, J. Faleskog, C.F. Shih, Cell model for nonlinear fracture analysis – II. Fracture- process calibration and verification. International Journal of Fracture, 89(1998)375-398,
[12] K. C. Koppenhoefer, R. H. Dodds Jr, Loading rate effects on cleavage fracture of pre-cracked CVN specimens: 3-D studies. Engineering Fracture Mechanics, 58 (1997) 249-270.
[13] A. Eberle, D. Klingbeil, W. Baer, P. Wossidlo, R. Liicker, The Calculation Of Dynamic

Jr-Curves From 2d And 3d Finite Element Analyses Of A Charpy Test Using A Rate-Dependent Damage Model, Elsevier Science Ltd, 2002.

[14] B. Tanguy, J. Besson, R. Piques, A. Pineau, Ductile to brittle transition of an A508 steel characterized by Charpy impact test. Part II: Modeling of the Charpy transition curve. Engineering Fracture Mechanics, 72(2005) 413-434.

[15] L. C. A. Folch, F. M. Burdekin, Application of coupled brittle-ductile model to study correlation between Charpy energy and fracture toughness values. Engineering Fracture Mechanics, 63(1999) 57-80.

[16] P. Thibaux, F. Van Den Abeele, Determination of crack initiation and propagation energy in instrumented Charpy V-notch impact tests by finite element simulations. Pipeline Technology Conference, Ostend, 2009, Ostend 209-093.

[17] C. K. A. Nonn, Modelling of Damage Behaviour of High Strength Pipeline Steel, Europipe, 2010. http://www.europipe.com/73-0-2000-2012.html

[18] S. Hong, S. Shin, S. Lee, N.J. Kim, Effects of specimen thickness and notch shape on fracture modes in the drop weight tear test of API X70 and X80 linepipe steels. Metallurgical and Materials Transactions A, 2011, Doi: 10.1007/s11661-011-0697-9.